# High energy, high resolution photoelectron spectroscopy of $Co_2Mn_{1-x}Fe_xSi$.

Gerhard H. Fecher, Benjamin Balke, Siham Ouardi, and Claudia Felser*

*Institut für Anorganische und Analytische Chemie,*

*Johannes Gutenberg - Universität, D-55099 Mainz, Germany.*

Eiji Ikenaga, Jung-Jin Kim, Shigenori Ueda, and Keisuke Kobayashi

*Japan Synchrotron Radiation Research Institute (SPring-8/JASRI),*

*Kouto 1-1-1, Sayo-cho, Sayou-gun, Hyogo, 679-5198, Japan*

(Dated: February 6, 2008)



## Abstract

This work reports on high resolution photoelectron spectroscopy for the valence band of $Co_2Mn_{1-x}Fe_xSi$ ($x = 0, 0.5, 1$) excited by photons of about 8 keV energy. The measurements show a good agreement to calculations of the electronic structure using the LDA+$U$ scheme. It is shown that the high energy spectra reveal the bulk electronic structure better compared to low energy XPS spectra. The high resolution measurements of the valence band close to the Fermi energy indicate the existence of the gap in the minority states for all three alloys.

PACS numbers: 79.60.Bm, 71.20.Lp, 71.20.Nr

Keywords: Heusler compounds, Photoelectron spectroscopy, Electronic Structure, Intermetallics.

*Electronic address: fecher@uni-mainz.de

## I. INTRODUCTION

Electronic devices exploiting the spin of an electron (spintronics [1]) have attracted great scientific interest in particular for magneto-electronics [2]. The basic element is a ferromagnetic electrode providing a spin polarised electrical current. Materials with a complete spin polarisation would be most desirable, i.e. a metal for spin up and an insulator for spin down electrons. Such materials are called half-metallic ferromagnets [3, 4]. Kübler *et al* [5] recognised that the minority-spin state density at the Fermi energy nearly vanishes in the Heusler compounds $Co_2MnAl$ and $Co_2MnSn$. The authors concluded that this should lead to peculiar transport properties in these compounds because only the majority density contributes. The Heusler alloy $Co_2MnSi$ has attracted particular interest because it is predicted to have a large minority spin band gap of 0.4 eV and, at 985 K, has one of the highest Curie temperatures, among the known Heusler compounds [6, 7]. An even higher Curie temperature (1100 K) accompanied by a large magnetic moment (6 $\mu_B$) was found in recent investigations of $Co_2FeSi$ [8, 9, 10]. The end members of the series $Co_2Mn_{1-x}Fe_xSi$, that are the purely Mn or Fe containing compounds, have been used for fabrication of magnetic tunnel junctions [11, 12]. The tunnel magneto-resistance ratios of 159% in the Mn compound at low temperature and 41% in the Fe compound at room temperature suggest that still an improvement in the materials is necessary for successful use in devices.

It was recently shown that the complete substitutional series $Co_2Mn_{1-x}Fe_xSi$ ($0 \leq x \leq 1$) orders in the Heusler type $L2_1$ structure [13]. Magneto-structural investigations using $^{57}$Fe Mößbauer spectroscopy confirmed the high degree of structural order. A structural phase transitions at about 1025 K was detected by means of differential scanning calorimetry. Low temperature magnetometry confirmed a Slater-Pauling like behaviour [14] of the complete series of alloys with the magnetic moment increasing linearly from 5 $\mu_B$ to 6 $\mu_B$ with increasing iron content $x$ from 0 to 1.

Photoelectron spectroscopy is one of the best suited techniques to study the occupied electronic structure of materials. Low kinetic energies result in a small electron mean free path of less than 5.2 Å at kinetic energies below 100 eV. That is, the escape depth of the electrons is less than one cubic cell of the investigated compounds and mainly the surface will contribute to the intensity if using UV light for excitation. This very high surface sensitivity may be able to explain the quite low spin polarisation of photoelectrons emerging

from single crystalline $Co_2MnSi$ films at the Fermi level of only 12 % [15]. Wang *et al* [15, 16] assumed that partial chemical disorder was responsible for this discrepancy with the theoretical predictions.

In the common X-ray photoelectron spectroscopy (XPS) one uses medium energies for excitation being provided by Al-$K_\alpha$ or Mg-$K_\alpha$ sources resulting in a probing depth of about 24 Å at 1.2 keV. The situation becomes much better at higher energies. In hard X-ray photoelectron spectroscopy with excitation energies of about 8 keV one will reach a high bulk sensitivity with an escape depth being larger than 115 Å (corresponding to 20 cubic cells). Lindau *et al* [17] demonstrated in 1974 the possibility of high energy photoemission with energies up to 8 keV, however, no further attention was devoted to such experiments for many years. High energy photoemission (at about 15 keV excitation energy) was also performed as early as 1989 [18] using a $^{57}$Co Mößbauer $\gamma$-source for excitation, however, with very low resolution only. Nowadays, high energy excitation and analysis of the electrons become easily feasible due to the development of high intense sources (insertion devices at synchrotron facilities) and multi-channel electron detection. Thus, high energy photoemission spectroscopy was recently introduced by several groups [19, 20, 21, 22, 23, 24] as a bulk sensitive probe of the electronic structure in complex materials.

In Ref. [25] it was demonstrated that high energy photoelectron spectroscopy is a useful tool to study the electronic structure of complex Heusler alloys using the example of $Co_2Cr_{0.6}Fe_{0.4}Al$. In that work photon energies of 3.5 keV were used for excitation, and compared to resonant, medium energy (0.5-0.8 keV) excitation at the $L_{3,2}$ edges of the contributing 3*d*-transition metals. In the present work, an excitation energy of $h\nu = 8$ keV was used to study the density of states of $Co_2Mn_{1-x}Fe_xSi$ with $x = 0, 0.5, 1$.

## II. EXPERIMENTAL AND COMPUTATIONAL DETAILS

$Co_2Mn_{1-x}Fe_xSi$ samples were prepared by arc melting of stoichiometric amounts of the constituents in an argon atmosphere at $10^{-4}$ mbar. Care was taken to avoid oxygen contamination. This was ensured by evaporating Ti inside of the vacuum chamber before melting the compound as well as by additional purifying of the process gas. After cooling of the resulting polycrystalline ingots, they were annealed in an evacuated quartz tube for 21 days. Rods with a dimension of $(1 \times 1 \times 5)$ mm$^3$ were cut from the ingots by spark-erosion for

experiments on in-situ fractured samples. Flat discs with about 10 mm diameter and 1 mm thickness were cut and polished for spectroscopic investigations. Further experimental details and results of the structural and magnetic properties are reported in Ref. [13, 26].

X-ray photoemission spectroscopy was used to verify the composition and to check the cleanliness of the samples. After removal of the native oxide from the polished surfaces by $Ar^+$ ion bombardment, no impurities were detected with XPS. The ESCALAB Mk II (VG) was also used to take valence band spectra at 1253.6 eV (Mg $K_\alpha$ with a natural line width of 0.69 eV [27]) for comparison. For this purpose, the slits and pass energy were set for an analyser-resolution of 200 meV. The energy was calibrated at the Au $4f_{7/2}$ emission line.

The electronic structure was explored experimentally by means of high energy X-ray photoemission spectroscopy (HXPS). The measurements were performed at the beamline BL47XU of SPring 8 (Hyogo, Japan). The photons are produced by means of a 140-pole in-vacuum undulator and are further monochromatised by two double-crystal monochromators. The first monochromator uses Si(111) crystals and the second a Si(111) channel-cut crystal with 444 reflections (for 8 keV X-rays). The energy of the photoemitted electrons is analysed using a Gammadata - Scienta R 4000-10kV electron spectrometer. The ultimate resolution of the set up (monochromator plus analyser at 50 eV pass energy using a 200 $\mu$m slit) is 83.5 meV at 7935.099 eV photon energy as employed for the reported experiments. Under the present experimental conditions an overall resolution of 250 meV has been reached for the valence band spectra and 130 meV for the spectra taken at the Fermi energy. All values concerning the resolution are determined from the Fermi-edge of an Au sample. Due to the low cross-section of the valence states from the investigated compounds, the spectra had to be taken with $E_{pass} = 200$ eV and a 500 $\mu$m (200 $\mu$m) slit for a good signal to noise ratio. The polycrystalline samples have been fractured in-situ before taking the spectra to remove the native oxide layer. Core-level spectra have been taken to check the cleanliness of the samples. No traces of impurities were found. The valence band spectra were collected over up to 4 h at about 100 mA electron current in the storage ring in the top-up mode. All measurements have been taken at a sample temperature of 20 K.

The self-consistent electronic structure calculations have been carried out using the full potential linearised augmented plane wave method (FLAPW) as provided by Wien2k [28]. The exchange-correlation functional was taken within the generalised gradient approximation (GGA) as introduced by Perdew *et al* [29]. A $25 \times 25 \times 25$ mesh has been used for

integration, resulting in 455 $k$-points in the irreducible wedge of the Brillouin zone of the primitive cell of the cubic compounds. All muffin tin radii have been set as nearly touching spheres with $r_{MT} = 2.29a_{0B}$ for the $3d$ elements and $2.15a_{0B}$ for Si ($a_{0B} = 0.529177$ Å). A structural optimisation for the compounds showed that the calculated lattice parameters deviate from the experimental ones only marginally [10]. Further details of the calculations and their results are reported in Reference [10, 13].

Partial cross sections have been calculated for better comparison of the calculated electronic structure with the valence band photoemission spectra. The orbital momentum and site resolved cross sections were calculated for atomic valence states using a modified relativistic Dirac-solver based on the computer programs of Salvat and Mayol [30, 31]. The radial integrals for the various transitions ($s \rightarrow p$, $p \rightarrow s, d$, and $d \rightarrow p, f$) have been computed using the dipole length-form. In addition, the electron mean free path was calculated using the Tanuma-Powell-Penn (TPP-2M) equations [32].

## III. RESULTS AND DISCUSSION

Figure 1 displays the calculated energy dependence of the atomic and orbital resolved cross sections together with the electron mean free path in $Co_2Mn_{0.5}Fe_{0.5}Si$. The shown data cover the range of kinetic energies observed in XPS and HXPS. In this energy range, the electron mean free path (Fig. 1(e)) varies nearly linearly with increasing kinetic energy and covers a range of escape depths from about 5 to 20 cubic Heusler cells. The calculated electron mean free path in the pure Mn or Fe containing compounds is very close to the one of the mixed compound as the physical properties (density, number and kind of valence electrons) entering the TPP-2M equations are almost the same.

At low energies (1 keV), like used in regular XPS, the partial cross section of the valence states is dominated by the $d$-states of the transition metal elements. This cross section decreases faster with increasing energy compared to that of the $s$ or $p$ states. At high energies (8 keV) the strongest cross sections is observed for the $s$-states, because the cross section of $p$ states also drops down faster with energy compared to $s$-states. Thus one expects a pronounced change of the photoemission intensities if going from XPS (1.2 keV) to HXPS (8 keV).

Figure 2 displays the calculated, spin resolved density of states for the investigated com-

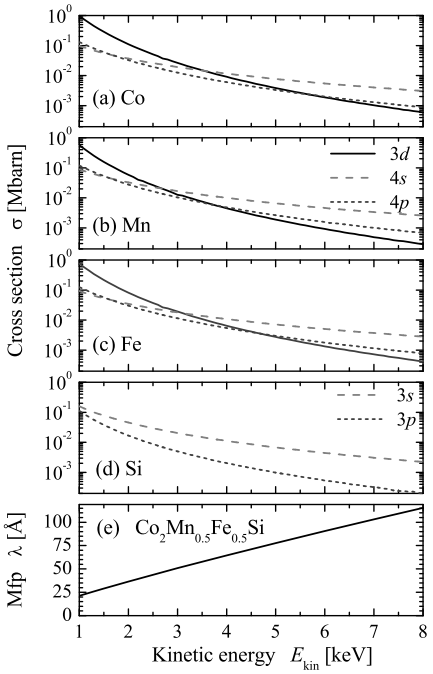


FIG. 1: Cross sections and electron mean free path.

The atomic, partial cross sections of the contributing elements are displayed in (a)-(d) and the electron mean free path (Mfp) as calculated for $Co_2Mn_{0.5}Fe_{0.5}Si$ in (e).

pounds. All three compounds, $Co_2Mn_{1-x}Fe_xSi$ with $x = 0, 1/2$, and 1, exhibit a clear gap in the minority density of states, that is they are half-metallic ferromagnets. The gap has the result that the calculated spin magnetic moments of $Co_2MnSi$ and CoFeSi have integer values of 5 $\mu_B$ and 6 $\mu_B$, respectively. The magnetic moment of $Co_2Mn_{1/2}Fe_{1/2}Si$ is 5.5 $\mu_B$. All those values are in perfect agreement with the experimental values [13] and the Slater-Pauling rule [14]. The majority spin density reveals that the $d$-states emerging from flat majority bands are shifted away from the Fermi energy $\epsilon_F$ with increasing Fe content. At the same time the Fermi energy moves from near the top of the minority valence states towards the bottom of the minority conduction bands. It is clearly visible that the gap in the minority states is defined by regions of high density emerging from flat $d$-bands. At the same time, the majority spin density contributes only few states in the region close to the Fermi energy. This behaviour is typical for Heusler compounds with high magnetic moments. More details of the electronic structure are reported in Refs. [10, 13].

The particular shape of the spin densities close to $\epsilon_F$ - a low density emerging from

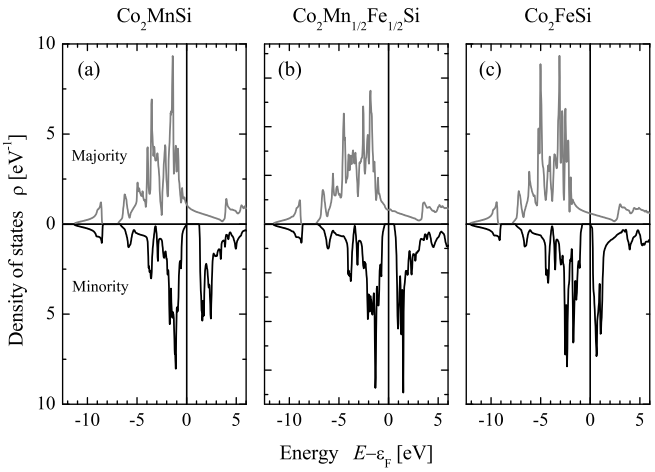


FIG. 2: Spin resolved density of states of $Co_2Mn_{1-x}Fe_xSi$ for $x = 0, 1/2$, and 1.

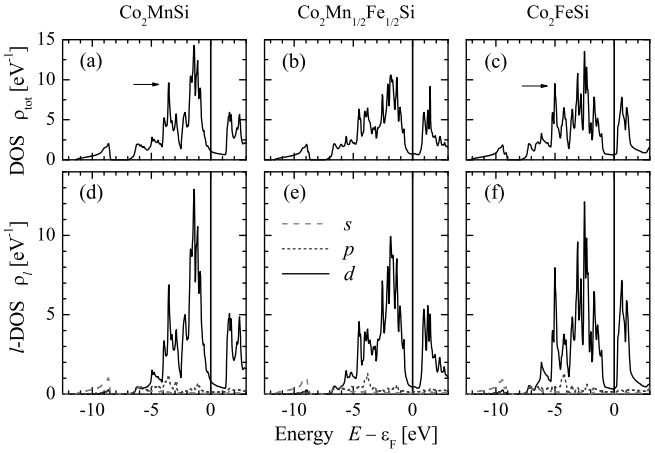


FIG. 3: Spin averaged density of states of $Co_2Mn_{1-x}Fe_xSi$.
The total, spin averaged density of states $\rho_{tot}$ is shown in (a) - (c) for $x = 0, 1/2$, and 1. The corresponding orbital momentum resolved $l$-DOS $\rho_l$ is displayed in (d) - (f).

majority states surrounded by regions of high minority density - should be easily detected in valence band photoemission and thus may be a good indicator for the existence of the gap, even without spin analysis. Figures 3(a)-(c) show the total, spin integrated density of states. The low density of states in the vicinity of the Fermi energy is clearly visible.

Additionally, the orbital momentum resolved density of states ($l$-DOS) is shown in Figure 3(d)-(f). The partial DOS of the interstitial can not be extracted from the calculations in an $l$-resolved way and therefore is not included. The $l$-DOS for higher angular momenta ($l$)

is omitted as they contribute only very few to the total density of states. From Figure 3(d)-(f) it follows that the $s$-states are mainly found at below 8.5 eV below $\epsilon_F$. The density at the Fermi energy is dominated by $d$-states. Although the density of $d$-states is already low at $\epsilon_F$, the $s$-like density is still at least one order of magnitude smaller. The density related to $p$-states is found from the bottom of the $d$-bands up to about 1 eV below $\epsilon_F$. This behaviour reflects the interaction between transition metal $d$-states with Si $p$-states. For better comparison with the measured photoemission spectra, the $l$-DOS has been weighted in the following by the partial cross sections. The sum of the weighted $l$-DOS has been additionally convoluted by the Fermi-Dirac distribution (300 K for XPS; 20 K for HXPS) and afterwards has been broadened by Gaussians of 0.7 eV (XPS) or 0.27 eV (HXPS) width to account roughly for the experimental resolution at excitation energies of 1.2 keV or 8 keV, respectively.

The valence band spectra excited by Mg $K_\alpha$ radiation are shown in Figure 4. All three spectra show a high intensity close to the Fermi energy. The low lying $sp$ band at 8 eV to 11 eV below $\epsilon_F$ is only weakly revealed. There is also no particular structure seen close to $\epsilon_F$. However, a closer inspection of the maximum intensity of the emission exhibits that it is shifted away from the Fermi energy in the Fe containing alloys (b,c). The maximum intensity is found at -1.3 eV, -1.46 eV, and -1.55 eV for $x = 0$, 0.5, and 1, respectively. This observation is in rough agreement with the density of states where the maximum of the majority density (as well as the total DOS) is also shifted to higher binding energies with increasing Fe content. It is also seen in the DOS weighted by the partial cross sections (dashed lines in Fig. 4) where the maximum of the intensity shifts from -1.48 eV for $x = 0$ to -2.85 eV for $x = 1$. Both values are in the calculations larger than those observed in the spectra. In particular, this suggests that the calculations shift the $d$-states in $Co_2FeSi$ to much below the Fermi energy, what may be prevented by using different values of $U_{eff}$ such that the Fermi energy comes closer to the top of the minority valence band [10].

The results from high energy photoemission are shown in Figure 5. The spectra of all three compounds reveal clearly the low lying $s$-states at about -11 eV to -9 eV below the Fermi energy, in well agreement to the calculated DOS. These low lying bands are separated from the high lying $d$-states by the Heusler-typical hybridisation gap being clearly resolved in the spectra as well as the calculated DOS. The size of this gap amounts typically to $\Delta E \approx 2$ eV in Si containing compounds.

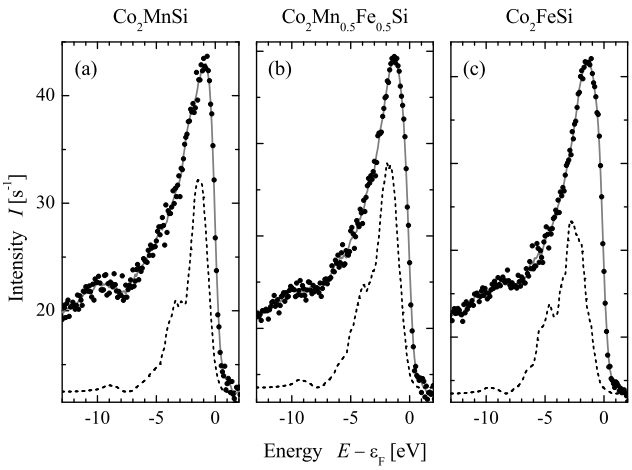


FIG. 4: Low energy valence band spectra of $Co_2Mn_{1-x}Fe_xSi$.
(a) - (c) display the XPS valence band spectra for $x = 0, 0.5$, and 1. The DOS - convoluted by the Fermi-Dirac distribution and weighted by the partial cross sections - is shown as dashed line. The spectra were excited by Mg $K_\alpha$ radiation (1.254 keV).

Obviously, the emission from the low lying $s$-states is pronouncedly enhanced compared to the emission from the $d$-states. This can be explained by a different behaviour of the cross sections of the $s$, $p$, and $d$ states with increasing kinetic energy as was recently demonstrated by Panaccione *et al* for the case of the silver valence band [23]. In particular, the cross section for $d$-states decreases faster with increasing photon energy than the one of the $s$-states. This behaviour influences also the onset of the $d$-bands at about -7 eV. Just at the bottom of those $d$-bands, they are hybridised with $s, p$-like states, leading to a relatively high intensity in this energy region.

The structure of the spectra in the range of the $d$ states agrees with the structures observed in the total DOS. However, one has to account not only for the experimental resolution but also for lifetime broadening if comparing that energy range. The lowest flat band of the majority band structure, accompanying the localised moment, results in a sharp peak in the DOS at about -3.5 eV and -5 eV for Mn and Fe, respectively (marked by arrows in Fig.3 (a) and (c). These peaks are shifted away from $\epsilon_F$ by the electron-electron correlation in the LDA+$U$ calculation and would appear without $U$ closer to the Fermi energy. Their energetic position corresponds to structures revealed in the measured spectra, thus they are a good proof for the use of the LDA+$U$ scheme.

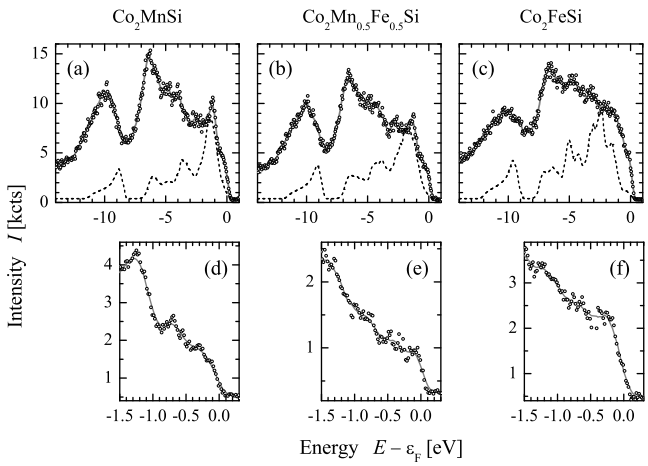


FIG. 5: High energy valence band spectra of $Co_2Mn_{1-x}Fe_xSi$.
The complete valence band is shown in panels (a) - (c) for $x = 0, 0.5$, and 1. The DOS - convoluted by the Fermi-Dirac distribution and weighted by the partial cross sections - is shown as dashed line. High resolution valence band spectra taken close to the Fermi energy are displayed in (d) - (f). The spectra were excited by synchrotron radiation with $h\nu = 7.939$ keV.

As mentioned, one also has to account for lifetime broadening. At 1.3 keV excitation, the emission is dominated by the high dense $d$-states at about -1.4 eV. Increasing the excitation energy to 8 keV (note the better resolution of set-up at that energy) has the result that the intensity in this energy range becomes considerably lower. At the same time, the emission from the remaining $d$-bands becomes strongly enhanced. Obviously, the intensity at the Fermi energy is much higher compared to the calculated DOS even after weighting by the partial cross sections. As those structures in the DOS emerge rather all from $d$-states, the transfer of the intensity maximum is not only explained by pure cross section effects. The valence band spectra may be seen as a convolution of the initial (bound) and final (unoccupied) state DOS. The final state DOS is rather constant at high kinetic energies and final state effects may play a minor rule only. Two other weighting factors enter the DOS-convolution. The first is, as explained above, the transition matrix element that contains both the selection rules and the cross sections (radial matrix elements). The radial matrix elements are partially responsible for the rearrangement of the orbital resolved intensities as discussed above. The second weighting factor is the complex self-energy of the photoelectron. Among other things, it depends on the hole lifetime due to the coupling of the photoemitted

electron with the hole left behind. At low kinetic energies, the spectra are obviously governed by the long life time of the holes at binding energies close to $\epsilon_F$. At high kinetic energies, where the sudden approximation is reached, the photoelectron is not as strongly coupled to its hole and the lifetime at $\epsilon_F$ plays less a role. Not only from the mean free path but also from the presented point of view, the high energy photoemission may help to understand the bulk electronic structure better than using only low energy XPS.

Most interesting is the behaviour of the calculated DOS and the measured spectra close to $\epsilon_F$ as this might give an advice about the gap in the minority states. The majority band structure contributes only few states to the density at $\epsilon_F$ emerging from strongly dispersing bands. This region of low density is enclosed by a high density of states arising from flat bands at the upper and lower limits of the minority band gap. The onset of the minority valence band is clearly seen in the total DOS as well as the low majority density at the Fermi energy. The same behaviour is principally observed in the measured valence band spectra as displayed in Figure 5(d)-(f). From the spectra, it can be estimated that the Fermi energy is in all three cases at least $\approx 0.5$ eV above the minority states with high density (see Fig. 2). This gives strong evidence that all compounds of the $Co_2Mn_{1-x}Fe_xSi$ series exhibit really half-metallic ferromagnetism. Actually it stays unexplained why there is a strong enhancement of the intensity emerging from the steep majority $d$-bands crossing the Fermi energy compared to the lower lying flat $d$-bands. The answer will need to use more sophisticated photoemission calculations that include the angular matrix elements to distinguish between $e_g$ and $t_{2g}$ states. However, such programs are presently not available for the high kinetic and photon energies as used in this work.

The values for $U_{eff}$ used here are the borderline cases for the half-metallic ferromagnetism over the complete series $Co_2Mn_{1-x}Fe_xSi$. They were used as being independent of the Fe concentration, what was suggested for Co from constrained LDA calculations. However, the valence band spectra indicate that the Fermi energy of both end members may fall inside of the minority gap rather than being located at the edges of the minority gap. This situation may be simulated by a variation of $U$. A comparison to the $U$-dependence of the minority gap shown in Ref.: [10] suggests smaller effective Coulomb exchange parameters for the Mn rich part and larger ones for the Fe rich part of the series. This might also explain the non-linearity reported in Ref. [13] for the hyperfine field. A variation of those parameters for all contributing $3d$ constituents in the calculations was omitted here because it would

not bring more insight into the nature of the problem, at present.

Overall, the measured photoelectron spectra agree well with the calculated density of states and principally verify the use of the LDA+$U$ scheme. In particular, the shape of the spectra close to $\epsilon_F$ can be explained by the occurrence of a gap in the minority states and thus points indirectly on the half-metallic state of all three compounds investigated here by photoemission. For clarity about the gap, spin resolved photoemission spectroscopy at high energies would be highly desirable. However, this will make another step of improvement of the instrumentation necessary, for both photon sources as well as electron energy and spin analysers, as the spin detection will need a factor of at least three to four orders of magnitude more intensity for a single energy channel at the same resolution as used here for the intensity spectra.

## IV. SUMMARY AND CONCLUSIONS

The quaternary Heusler compound $Co_2Mn_{1-x}Fe_xSi$ was investigated for $x = 0, 0.5, 1$. All samples of the substitutional series exhibit an $L2_1$ order, independent of the Fe concentration. In agreement with the expectation from the Slater-Pauling curve for half-metallic ferromagnets, the magnetic moment increases linearly with $x$ from 5 $\mu_B$ to 6 $\mu_B$.

True bulk sensitive, high energy photoemission bearded out the inclusion of electron-electron correlation in the calculation of the electronic structure and gave an indirect advise on the gap in the minority states. The valence band spectra indicate an increase of the effective Coulomb exchange parameters with increasing Fe concentration.

**Acknowledgment :**

The authors are grateful for the support by G. Schönhense and thank S. Wurmehl for preparing the $Co_2FeSi$ sample and H. C. Kandpal for help with the calculations. The synchrotron radiation experiments were performed at the beamline BL47XU of SPring-8 with the approval of the Japan Synchrotron Radiation Research Institute (JASRI) (proposal no. 2006A1476). This work was partially supported by a Grant-in-Aid for Scientific Research (A) (No.15206006), and also partially supported by a Nanotechnology Support Project, of The Ministry of Education, Culture, Sports, Science and Technology of Japan. Financial

support by the Deutsche Forschungsgemeinschaft (project TP7 in research group FG 559) is gratefully acknowledged.

---

[1] S. A. Wolf, D. D. Awschalom, R. A. Buhrman, J. M. Daughton, S. v. Molnar, M. L. Roukes, A. Y. Chtchelkanova, and D. M. Treger, Science **294**, 1488 (2001).

[2] G. A. Prinz, Science **282**, 1660 (1998).

[3] R. A. d. Groot, F. M. Mueller, P. G. v. Engen, and K. H. J. Buschow, Phys. Rev. Lett. **50**, 2024 (1983).

[4] J. M. D. Coey, M. Venkatesan, and M. A. Bari (Springer, Heidelberg, 2002), vol. 595 of *Lecture Notes in Physics*.

[5] J. Kübler, A. R. Williams, and C. B. Sommers, Phys. Rev. B **28**, 1745 (1983).

[6] S. Fuji, S. Sugimura, S. Ishida, and S. Asano, J. Phys.: Condens. Matter **2**, 8583 (1990).

[7] P. J. Brown, K.-U. Neumann, P. J. Webster, and K. R. A. Ziebeck, J. Phys.: Condens. Matter **12**, 1827 (2000).

[8] S. Wurmehl, G. H. Fecher, H. C. Kandpal, V. Ksenofontov, C. Felser, H.-J. Lin, and J. Morais, Phys. Rev. B **72**, 184434 (2005).

[9] S. Wurmehl, G. H. Fecher, H. C. Kandpal, V. Ksenofontov, C. Felser, and H.-J. Lin, Appl. Phys. Lett. **88**, 032503 (2006).

[10] H. C. Kandpal, G. H. Fecher, and C. Felser, Phys. Rev. B **73**, 094422 (2006).

[11] K. Inomata, S. Okamura, A. Miyazaki, M. Kikuchi, N. Tezuka, M. Wojcik, and E. Jedryka, J Phys. D: Appl. Phys. **39**, 816 (2006).

[12] M. Oogane, Y. Sakuraba, J. Nakata, H. Kubota, Y. Ando, A. Sakuma, and T. Miyazaki, J Phys. D: Appl. Phys. **39**, 834 (2006).

[13] B. Balke, G. H. Fecher, H. C. Kandpal, C. Felser, K. Kobayashi, E. Ikenaga, J.-J. Kim, and S. Ueda, Phys. Rev. B **74**, 104405 (2006).

[14] G. H. Fecher, H. C. Kandpal, S. Wurmehl, and C. Felser, J. Appl. Phys. **99**, 08J106 (2006).

[15] W. H. Wang, M. Przybylskia, W. Kuch, L. I. Chelaru, J. Wang, Y. F. Lu, J. Barthel, and J. Kirschner, J. Magn. Magn. Mat. **286**, 336 (2005).

[16] W. H. Wang, M. Przybylski, W. Kuch, L. I. Chelaru, J. Wang, F. Lu, J. Barthel, H. L. Meyerheim, and J. Kirschner, Phys. Rev. B **71**, 144416 (2005).

[17] I. Lindau, P. Pianetta, S. Doniach, and W. E. Spicer, Nature **250**, 214 (1974).

[18] W. Meisel, Hyperfine Interact. **45**, 73 (1989).

[19] K. Kobayashi, M. Yabashi, Y. Takata, T. Tokushima, S. Shin, K. Tamasaku, D. Miwa, T. Ishikawa, H. Nohira, T. Hattori, et al., Appl. Phys. Lett. **83**, 1005 (2003).

[20] A. Sekiyama and S. Suga, J. Electron Spectrosc. Relat. Phenom. **137-140**, 681 (2004).

[21] S. Thiess, C. Kunz, B. C. C. Cowie, T.-L. Lee, M. Reniera, and J. Zegenhagen, Solid State Comm. **132**, 589 (2004).

[22] K. Kobayashi, Nucl. Instrum. Methods Phys. Res., Sect. A **547**, 98 (2005).

[23] G. Panaccione, G. Cautero, M. Cautero, A. Fondacaro, M. Grioni, P. Lacovig, G. Monaco, F. Offi, G. Paolicelli, M. Sacchi, et al., J. Phys.: Condens. Matter **17**, 2671 (2005).

[24] P. Torelli, M. Sacchi, G. Cautero, M. Cautero, B. Krastanov, P. Lacovig, P. Pittana, R. Sergo, R. Tommasini, A. Fondacaro, et al., Rev. Sci. Instrum. **76**, 023909 (2005).

[25] S. Wurmehl, G. H. Fecher, K. Kroth, F. Kronast, H. A. Dürr, Y. Takeda, Y. Saitoh, K. Kobayashi, H.-J. Lin, G. Schönhense, et al., J. Phys. D: Appl. Phys. **39**, 803 (2006).

[26] M. Kallmayer, H. J. Elmers, B. Balke, S. Wurmehl, F. Emmerling, G. H. Fecher, and C. Felser, J. Phys. D: Appl. Phys. **39**, 786 (2006).

[27] M. S. Banna and D. A. Shirley, J. Electron Spectrosc. Relat. Phenom. **8**, 23, 255 (1976).

[28] P. Blaha, K. Schwarz, G. K. H. Madsen, D. Kvasnicka, and J. Luitz, *WIEN2k, An Augmented Plane Wave + Local Orbitals Program for Calculating Crystal Properties* (Karlheinz Schwarz, Techn. Universitaet Wien, Wien, Austria, 2001).

[29] J. P. Perdew, K. Burke, and M. Ernzerhof, Phys. Rev. Lett. **77**, 3865 (1996).

[30] F. Salvat and R. Mayol, Comp. Phys. Commun. **62**, 65 (1991).

[31] F. Salvat and R. Mayol, Comp. Phys. Commun. **74**, 358 (1993).

[32] S. Tanuma, C. J. Powell, and D. R. Penn, Surf. Interf. Anal. **21**, 165 (1993).